Progress In Electromagnetics Research Letters, Vol. 43, 191–199, 2013

REALIZATION OF MICROSTRIP BANDPASS FILTER BALUN USING DOUBLE-SIDED PARALLEL-STRIP LINE WITH NOVEL COUPLING SCHEME

Cui-Hua Li[1, *] and Min-Quan Li[2]

[1]Department of Electronic Information and Electrical Engineering, Hefei University, Hefei 230601, China

[2]Key Laboratory of Intelligent Computing and Signal Processing, Ministry of Education, Anhui University, Hefei 230039, China

Abstract—In this paper, we propose a microstrip filter balun adopting double-sided parallel-strip line (DSPSL) with a conductor plane inserted in the middle of the substrate. Fed by the DSPSL at input port, two microstrip filters on top and bottom layers are excited simultaneously, with the frequency-independent out-of-phase feature obtained between two output ports. The proposed filter balun exhibits excellent performance with good frequency selectivity because of multiple transmission zeros generated by a new coupling scheme. Finally, a filter balun sample is designed and fabricated, and good agreement is obtained between its measured and simulated S-parameters.

1. INTRODUCTION

In modern wireless and communication systems, a balun is a crucial component highly demanded, which can be used to convert a balanced signal to an unbalanced one, or vice versa [1]. Balun and bandpass filter are cascaded directly for the aim of converting signals between an unbalanced and a balanced structure, and exhibits bandpass response simultaneously. It leads to high insertion loss and large area. For solving the problem, it turns out to be a good idea to integrate two separate circuit topologies into one device [2–6]. Because of multilayer configurations, the LTCC-based balun filters have compact sizes, but the structure and design procedure is very complicated [2]. On the

Received 23 September 2013, Accepted 12 November 2013, Scheduled 14 November 2013
* Corresponding author: Cui-Hua Li (chualimw@gmail.com).

other hand, a symmetrical four-port balanced to unbalanced filter can be converted to a three port balun filter with one of the ports being opened [3]. Dual-mode ring resonators are introduced into balun filter designs for size reduction, however, their frequency selectivity is relative worse [5, 6].

The double-sided parallel-strip line (DSPSL), as a good transmission structure, is a suitable candidate for the balun design due to its inherent frequency-independent out-of-phase feature. In addition, it possesses advantage of easy realization of lines with various characteristic impedances compared to the conventional balanced transmission structure [7]. Many different types of microwave components have been designed by researchers using DSPSL [8–10]. DSPSL has been introduced to filter balun design for size reduction [11], and two transmission zeros exist around the passband.

In this paper, we present a bandpass filter balun based on DSPSL. Two separate bandpass filters on upper and lower layers are excited at the same time by the DSPSL. In geometry, they are symmetrical and the structure is compact because of double-layer configurations. A new third-order coupling scheme is proposed to achieve stringent frequency selectivity by generating multiple transmission zeros. Measured results exhibiting excellent filtering and balun performance are in good agreement with the simulated one.

2. FILTER BALUN DESIGN

2.1. Analysis of the New Coupling Scheme

In order to improve the frequency selectivity of the filter, cross coupling and source-load coupling are effective methods to generate finite attenuation poles next to the passband [12–15]. Some novel coupling schemes are presented for generating transmission zeros [16]. Figure 1 shows a third-order coupling scheme developed from the topology of Figure 1(f) in [16]. Resonators 1, 2, 3 represent three single-mode resonators.

It is well known that only single transmission zero can be obtained in conventional third-order cross coupled microstrip filter [14]. However, based on the coupling scheme proposed in Figure 1, we can realize a third-order quasi-elliptic filter. Here, the bandwidth and center frequency of the filter are set to be 210 MHz and 2.95 GHz, respectively. For filter physical realization, coupling coefficients M at its center frequency is given by: $M_{S1} = 1.02$, $M_{S2} = 0.15$, $M_{SL} = 0.012$, $M_{13} = 1.1$, $M_{23} = -1.1$, $M_{2L} = 1.21$.

The simulated frequency-dependent S-parameters of the filter corresponding to the coupling coefficients with different values of M_{SL}

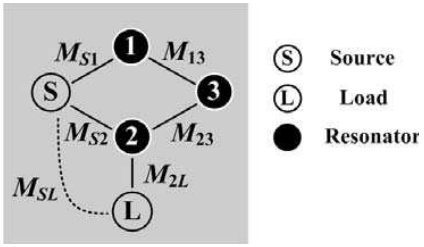

Figure 1. Layout of the proposed coupling scheme.

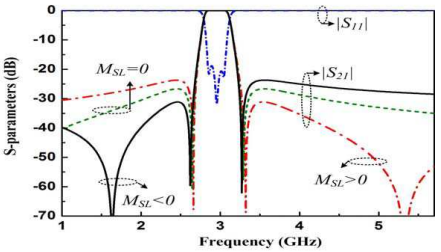

Figure 2. Simulated S-parameters of coupling coefficients with and without source-load coupling, respectively.

are plotted in Figure 2. When source-load coupling is not introduced, we can obtain quasi-elliptic function transmission response, with the two transmission zeros located at

$$\Omega = \frac{a \pm b}{2M_{S2}} \tag{1}$$

where $a = -M_{S2}(M_{33} + M_{11})$, $b = [M_{S2}^2(M_{33}^2 + M_{11}^2 + 4M_{13}^2 - 2M_{11}M_{33}) - 4M_{S1}M_{S2}M_{23}M_{13}]^{1/2}$.

When the source-load coupling is introduced into the third-order coupling scheme, the locations of two previous transmission zeros do not change. An additional transmission zero will be generated either at the higher stopband or the lower stopband depending on the sign of the source-loading coupling M_{SL}.

2.2. Characteristic Impedance of DSPSL

Figure 3(a) shows a three-dimensional view of the DSPSL with an inserted conductor plane which in fact behaves as a virtual ground and converts DSPSL into two separate back-to-back microstrip lines. The sketches of DSPSL and microstrip line are presented in Figures 3(b) and (c), respectively. According to the analysis in [11], we can get the characteristic impedances relationship between DSPSL and microstrip line of the same width as follows:

$$Z_1 = 2Z_2 \tag{2}$$

From the above Equation (2), we can easily calculate the characteristic impedance of the DSPSL in Figure 3(b) based on the microstrip line in Figure 3(c).

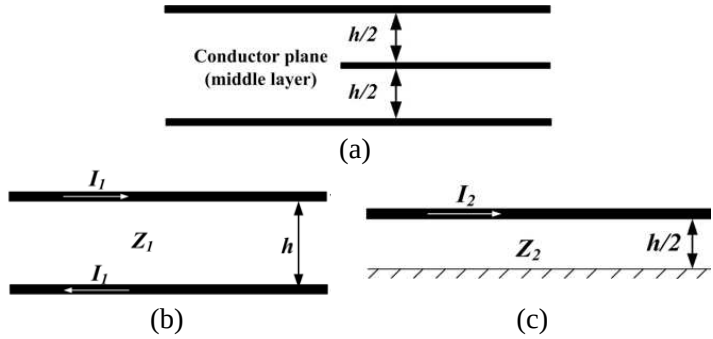

Figure 3. (a) DSPSL with an inserted conductor plane, and the schematic diagram of (b) DSPSL and (c) microstrip line.

2.3. Implementation of the Balun Filter with DSPSL

Figure 4 shows the configuration of the proposed filter balun. DSPSL is fed at the input port, two identical third-order bandpass filters with new coupling scheme on top layer and bottom layer are excited simultaneously. They are symmetrical in structure which results in the input energy separated in equal amounts. Meanwhile, the phase difference is theoretically perfect 180° because of the DSPSL-fed structure at port 1. As a result, an integrated bandpass filter balun is successfully constructed, which has several advantages such as size reduction, easy fabrication, good performance and so on, as compared with that using the conventional design methods by cascading two individual components-balun and filter.

The detailed structure of the third-order filter on top layer is presented in Figure 5, where resonators 1, 2, 3 represent the counterpart in Figure 1. The simulated S_{21}-parameters as a function of frequency for different values of L_d are plotted in Figure 6(a). The

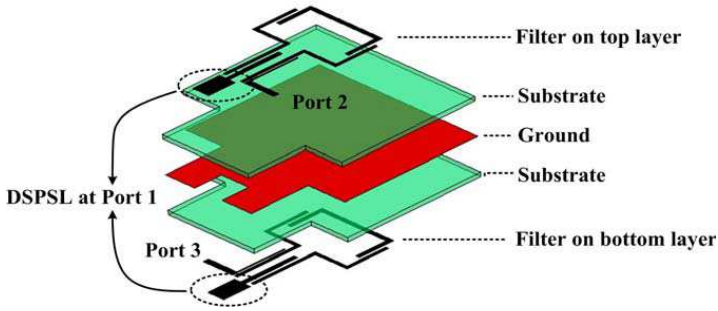

Figure 4. 3-D view of the proposed filter balun.

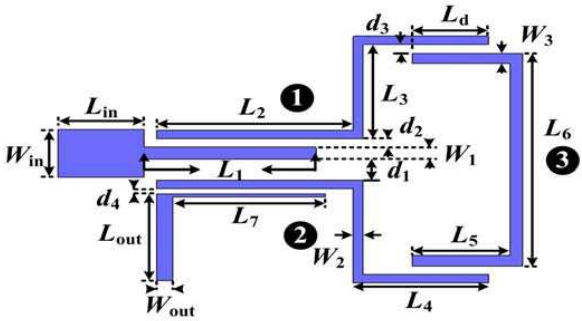

Figure 5. Detailed structure of the third-order filter on top layer.

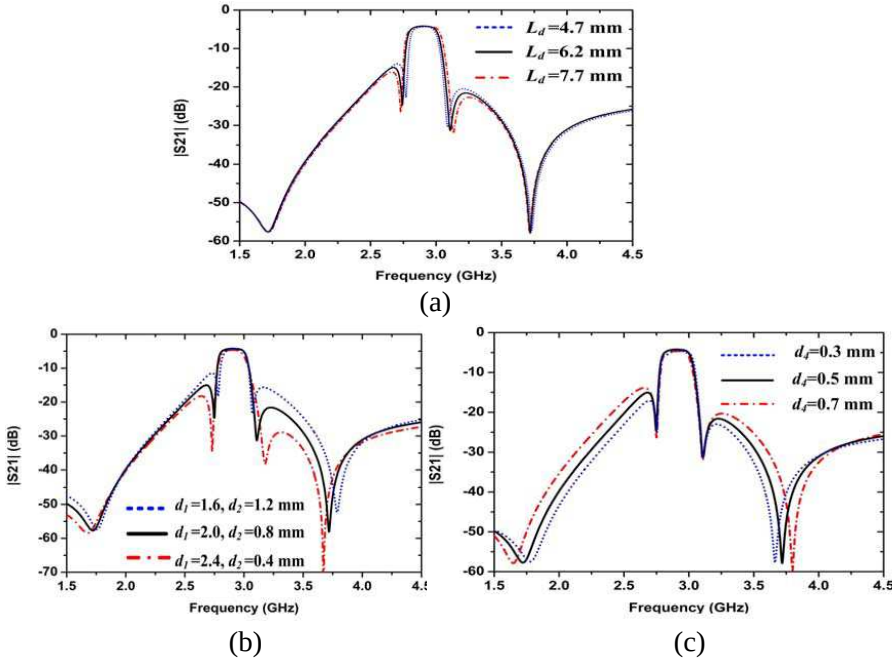

Figure 6. Simulated S_{21}-parameter as a function of frequency for different values of (a) L_d, (b) d_1 and d_2, and (c) d_4, respectively.

simulated S_{31}-parameters are omitted for the reason that they nearly coincide with S_{21}-parameters. The bandwidth of the filter increases with increasing L_d for stronger coupling.

The locations of the two transmission zeros next to the passband are dominated by the value of M_{S1} and M_{S2}. The resonators 1 and 2

are both excited by the DSPSL based on Figure 1. The different coupling strengths between the DSPSL and two resonators can be determined by the parameters d_1 and d_2. Figure 6(b) shows the simulated transmission response for different values of d_1 and d_2. The two transmission zeros move towards the passband with d_1 decreasing and d_2 increasing. The parameter d_4 can be used to determine the external Q-factor. When the value of d_4 decreases, the outer two transmission zeros will move towards the passband as demonstrated in Figure 6(c). The whole structure is finely optimized so as to meet our specifications, which is performed using the High Frequency Structure Simulator of HFSS.

3. RESULTS AND DISCUSSION

To validate our design, a filter balun sample was fabricated on a multilayer PCB technology with relative permittivity, loss tangent and thickness of each layer of 2.65, 0.0035 and 1 mm, respectively. The electrical conductivity and thickness of metal layer are 6.1×10^7 S/m and 0.0175 mm, respectively. The photograph of the proposed balun filter is demonstrated in Figure 7, and its size is $41.0 \times 30.0\,\text{mm}^2$. The geometrical parameters of filter are listed as follows (unit: mm): $W_1 = 1.1$, $W_2 = 0.8$, $W_3 = 1$, $W_4 = 0.5$, $W_{in} = 4.5$, $W_{out} = 2.65$, $L_{in} = 7$, $L_{out} = 8$, $L_1 = 15$, $L_2 = 16$, $L_3 = 9$, $L_4 = 11$, $L_5 = 8$, $L_6 = 20.3$, $L_d = 6.4$, $d_1 = 2$, $d_2 = 0.8$, $d_3 = 0.8$, and $d_4 = 0.5$.

As shown in Figure 8(a), the measured center frequency and bandwidth of the balun filter are around 2.95 GHz and 250 MHz, respectively. Besides, the measured insertion loss including SMA connectors is about $(3 + 1.4)$ dB, and return loss in the passband is better than 10 dB. We acquired multiple transmission zeros located at 2, 2.8, 3.2 and 3.7 GHz. Compared with the simulated S-parameters of its coupling scheme, the extra finite transmission zero located in the lower stopband is for the frequency-variant external coupling brought

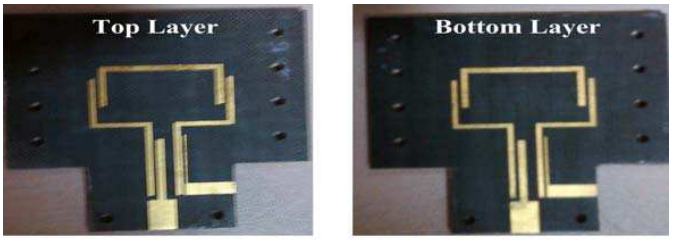

Figure 7. The photograph of the proposed balun filter.

by the exciting ways in Figure 4. Furthermore, Figure 8(b) shows that the measured in-band phase difference is within $180° \pm 5°$, and the amplitude difference is within ± 0.5 dB.

In the measurement, the central probe of the SMA connector is soldered on the top strip of DSPSL while the outer conductor is soldered on the bottom strip of DSPSL. The outer conductor of SMA on port 1 is isolated from the ground of SMA connectors of the other two ports. This will result in slight performance deterioration. For further application, a global ground for all ports can be introduced to solve the problem. The frequency shift is mainly due to the fabrications tolerances and the alignment of two substrate boards.

Table 1 compares measured bandwidths, minimum insertion losses and transmission zeros for published and our prototype balun filters. We can see that the proposed balun filter has lower insertion loss in the passband and better frequency selectivity due to more transmission zeros.

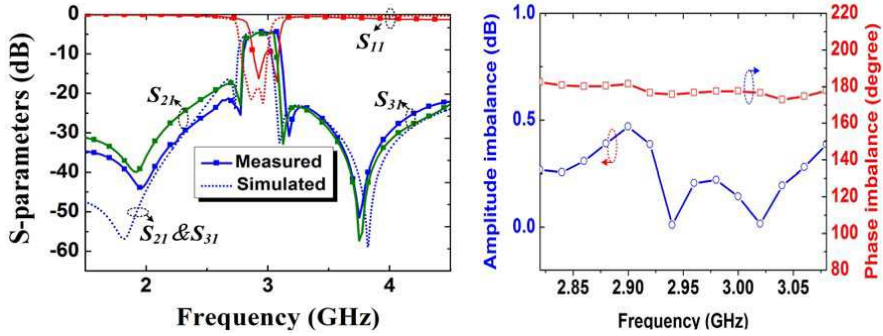

Figure 8. (a) Simulated and measured S-parameters of the proposed filter balun, and (b) its measured amplitude and phase imbalances.

Table 1. Comparison with the balun filters presented in references.

Techniques	FBW and Center frequency (GHz)	IL (dB)	Number of TZ below and above passband
Multilayer LTCC [1]	8% and 20.5	3.0	1 and 0
Four-port SIR [3]	10% and 0.9	2.28	1 and 1
Dual mode ring resonator [4]	18.7% and 2.57	2.5	1 and 1 (S_{21}) 0 and 0 (S_{31})
DSPSL [11]	7% and 0.985	1.5	1 and 1
This work	8.5% and 2.95	1.4	2 and 2

4. CONCLUSION

In this paper, we propose a novel balun filter using DSPSL with a new coupling scheme. This component can not only behave as a balanced-to-unbalanced converter, but also as a bandpass filter. The DSPSL ensures the out-of-phase feature between two output ports. Adopting the proposed coupling topology, multiple transmission zeros can be obtained to improve frequency selectivity. The filter balun was fabricated based on standard printed circuit board (PCB) technique, with good agreement obtained between its measured and simulated S-parameters.

ACKNOWLEDGMENT

This work was supported by the Outstanding Young Talent Foundation of Anhui Province, the Hefei University Foundation under Grant 10KY03ZR, and the NSF under Grant KJ2011A007 and 1208085MF104 of Anhui Province.

REFERENCES

1. Chiu, L., T. Y. Yum, Q. Xue, and C. H. Chan, "A wideband compact parallel-strip 180 Wilkinson power divider for push-pull circuitries," *IEEE Microw. Wireless Compon. Lett.*, Vol. 16, No. 1, 49–51, Jan. 2006.
2. Yeung, L. K. and K. L. Wu, "An LTCC balanced-to-unbalanced extracted-pole bandpass filter with complex load," *IEEE Trans. Microw. Theory Tech.*, Vol. 54, No. 4, 1512–1518, Apr. 2006.
3. Wu, C. H., C. H. Wang, S. Y. Chen, and C. H. Chen, "Balanced-to-unbalanced bandpass filters and the antenna application," *IEEE Trans. Microw. Theory Tech.*, Vol. 56, No. 11, 2474–2482, Nov. 2008.
4. Jung, E. Y. and H. Y. Hwang, "A balun-BPF using a dual-mode ring resonator," *IEEE Microw. Wireless Compon. Lett.*, Vol. 17, No. 9, 652–654, Sep. 2007.
5. Sun, S. and W. Menzel, "Novel dual-mode balun bandpass filters using cross-slotted patch resonator," *IEEE Microw. Wireless Compon. Lett.*, Vol. 21, No. 8, 415–417, Aug. 2011.
6. Cheong, P., T. S. Lv, W. W. Choi, and K. W. Tam, "A compact microstrip square-loop dual-mode balun-bandpass filter with simultaneous spurious response suppression and differential

performance improvement," *IEEE Microw. Wireless Compon. Lett.*, Vol. 21, No. 2, 77–79, Feb. 2011.

7. Kim, S. G. and K. Chang, "Ultrawide-band transitions and new microwave components using double-sided parallel-strip lines," *IEEE Trans. Microw. Theory Tech.*, Vol. 52, No. 9, 2148–2151, Sep. 2004.
8. Shi, J., J. X. Chen, and Q. Xue, "A novel differential bandpass filter based on double-sided parallel-strip line dual-mode resonator," *Microw. Opt. Tech. Lett.*, Vol. 50, No. 7, 1733–1735, Jul. 2008.
9. Chen, J. X., K. W. Lau, C. H. K. Chin, Q. Xue, and C. H. Chan, "A double-sided parallel-strip line push-pull oscillator," *IEEE Microw. Wireless Compon. Lett.*, Vol. 18, No. 5, 335–337, May 2008.
10. Chen, J. X. and Q. Xue, "Novel 5 : 1 unequal Wilkinson power divider using offset double-sided parallel-strip lines," *IEEE Microw. Wireless Compon. Lett.*, Vol. 17, No. 3, 175–177, Mar. 2007.
11. Chen, J. X., C. Y. Cheung, and Q. Xue, "Integrated bandpass filter balun based on double-sided parallel-strip line with an inserted conductor plane," *Proceedings of Asia-Pacific Microw. Conf.*, 1–4, 2007.
12. Fan, J. W., C. H. Liang, and X. W. Dai, "Design of cross-coupled dual-band filter with equal-length split-ring resonators," *Progress In Electromagnetics Research*, Vol. 75, 285–293, 2007.
13. Kuo, J. T., S. C. Tang, and S. H. Lin, "Quasi-elliptic function bandpass filter with upper stopband extension and high rejection level using cross-coupled stepped-impedance resonators," *Progress In Electromagnetics Research*, Vol. 114, 395–405, 2011.
14. Hong, J. S. and M. J. Lancaster, "Microstrip cross-coupled trisection bandpass filters with asymmetric frequency characteristics," *IEE Proc. — Microw. Antennas Propag.*, Vol. 146, No. 1, 84–90, Feb. 1999.
15. Ho, M. H. and P. F. Chen, "Suspended substrate stripline bandpass filters with source-load coupling structure using lumped and full-wave mixed approach," *Progress In Electromagnetics Research*, Vol. 122, 519–535, 2012.
16. Rosenberg, U. and S. Amari, "Novel coupling schemes for microwave resonator filters," *IEEE Trans. Microw. Theory Tech.*, Vol. 50, No. 12, 2896–2902, Dec. 2002.